International Journal of Bifurcation and Chaos, Vol. 11, No. 6 (2001) 1645–1653

EXACT NUMBER OF MOSAIC PATTERNS IN CELLULAR NEURAL NETWORKS

JUNG-CHAO BAN, SONG-SUN LIN* and CHIH-WEN SHIH*,†
Department of Applied Mathematics, National Chiao Tung University, Hsinchu, Taiwan, R.O.C.

Received February 10, 2000; Revised December 15, 2000

This work investigates mosaic patterns for the one-dimensional cellular neural networks with various boundary conditions. These patterns can be formed by combining the basic patterns. The parameter space is partitioned so that the existence of basic patterns can be determined for each parameter region. The mosaic patterns can then be completely characterized through formulating suitable transition matrices and boundary-pattern matrices. These matrices generate the patterns for the interior cells from the basic patterns and indicate the feasible patterns for the boundary cells. As an illustration, we elaborate on the cellular neural networks with a general 1×3 template. The exact number of mosaic patterns will be computed for the system with the Dirichlet, Neumann and periodic boundary conditions respectively. The idea in this study can be extended to other one-dimensional lattice systems with finite-range interaction.

1. Introduction

The cellular neural network (CNN) proposed by Chua and Yang [1988a, 1988b] is a large aggregation of analogue circuits. The system presents itself as an array of identical cells C_i which are locally coupled. In this study, we consider the CNN with cells coupled in a one-dimensional fashion (1-d CNN). Assume that the cells are sitting on the lattice $T_n := \{i \in \mathbf{Z}^1 | 1 \le i \le n\}$. The governing equation for the cell C_i at the site i, $i \in T_n$, takes the form

$$\frac{dx_i}{dt} = -x_i + \sum_{1 \le |k| \le r} \beta_k f(x_{i+k}) + af(x_i) + z\,, \quad (1)$$

where x_{i+k}, $i + k \notin T_n$, satisfies certain boundary condition to be described below. Herein, the output function f is a piecewisely linear function given by

$$f(\xi) = \frac{1}{2}(|\xi + 1| - |\xi - 1|)\,,$$

and $y_i = f(x_i)$ is the output for the cell at i. In addition, z is a time-independent bias and r is a positive integer indicating the radius of connection between cells. The coupling parameters β_k and a constitute a space-invariant $1 \times (2r + 1)$ template A_r. Namely,

$$A_r = [\beta_{-r} \cdots \beta_{-1} \quad a \quad \beta_1 \cdots \beta_r]\,.$$

We denote by $N_r(i) = \{k | i - r \le k \le i + r\}$ the neighbors of the cell C_i, which are within the range of connection for C_i. A practical CNN has finitely many cells. Hence, the boundary condition (B.C.) has to be imposed and realized. We shall consider three types of boundary conditions in this presentation; namely, the Dirichlet, Neumann and periodic boundary conditions. These conditions are illustrated for 1-d CNN with $r = 1$ as follows.

Dirichlet B.C.:

The absent cell x_0 (resp. x_{n+1}) on the left-hand side

*The authors are supported, in part, by the National Science Council of Taiwan, R.O.C.
†Author for correspondence.
E-mail: cwshih@math.nctu.edu.tw

of x_1 (resp. the right-hand side of x_n) are set to constants. Namely,

$$x_0(t) = \tilde{x}_0\,, \quad x_{n+1}(t) = \tilde{x}_{n+1}\,.$$

The situation that the imposed boundary data $\tilde{x}_0$ and $\tilde{x}_{n+1}$ have their absolute values greater than one is represented by D_1-B.C., while the case $\tilde{x}_0 = \tilde{x}_{n+1} = 0$ is denoted by D_0-B.C.

Neumann B.C.:

It is the zero-flux or reflective B.C., i.e.

$$x_0(t) = x_1(t)\,, \quad x_{n+1}(t) = x_n(t)\,.$$

Periodic B.C.:

Two ends of T_n are connected to form a circular array. Namely,

$$x_0(t) = x_n(t)\,, \quad x_{n+1}(t) = x_1(t)\,.$$

Let $x = (x_1, x_2, \ldots, x_n)$ be a stationary solution of (1). The associated output $y = (y_1, y_2, \ldots, y_n)$ with $y_i = f(x_i)$ is called a (stationary) pattern. The stationary solutions and patterns can be classified into four types: mosaic, defect, interior, and transitional, as defined in [Juang & Lin, 2000]. Herein, the definitions of the mosaic solutions and patterns which are the main concerns in this work are recalled. They are slightly modified to fit in the context of this study, that is, on the solutions and patterns on "finite" lattice.

Definition 1.1. A stationary solution $x = (x_1, x_2, \ldots, x_n)$ of (1) is called a *mosaic solution* if $|x_i| > 1$ for all $i \in T_n$. Its associated (output) pattern is called a *mosaic pattern*.

Notably, the mosaic solutions of CNN were called stable system equilibrium points in [Chua & Yang, 1988]. These mosaic solutions are all stable on finite lattice and on infinite lattice. Furthermore, under certain conditions on the parameters, every solution tends to a mosaic solution as time tends to positive infinity, cf. [Lin & Shih, 1999]. Our approach of constructing mosaic patterns on T_n for (1) is to combine the basic patterns and form patterns on larger lattices, as discussed in [Shih, 1998] and [Juang & Lin, 2000]. The notation $I[k, l] = \{k, k+1, \ldots, l\}$ will be used in the following discussion. It represents the set of all integers that are no smaller than k and no greater than l, for any two integers $k < l$.

Definition 1.2. A *basic* (*mosaic*) *solution* (corresponding to template A_r) is an $(2r+1)$-tuple $(x_1, x_2, \ldots, x_{2r+1})$ with $|x_i| > 1$ for $i \in I[1, 2r+1]$ and satisfies the $(r+1)$-th component of the stationary equation associated with (1). The output pattern corresponding to a basic solution is called a *basic pattern*.

Notably, in discussions of patterns on infinite lattice, a set T was called *basic* if $T = N_r(i)$ for some i, cf. [Shih, 1998] and [Juang & Lin, 2000]. The basic patterns as defined can also be viewed as the restrictions (or projections) of global mosaic patterns on the basic sets. The sites $i \in T_n$ with $N_r(i)$ not contained in T_n are called *boundary sites*. The collection of all boundary sites is denoted by **b**. As we shall see in the next section, the basic patterns can be directly determined from Eq. (1). Our scheme for constructing mosaic patterns on T_n can be described by three steps: (i) derive the feasible basic patterns in each parameter region, (ii) attach these basic patterns and form the patterns of the interior cells, (iii) match the boundary condition. This scheme can be implemented through formulating suitable transition matrices and the so-called boundary-pattern matrices. These formulations completely characterize the mosaic patterns for (1) with the above-mentioned boundary conditions. As a consequence, the number of mosaic patterns for every set of parameters can be exactly computed. Thus, our approach has also provided a systematic algorithm for computing the number of mosaic patterns. The results regarding the number of mosaic patterns in [Thiran *et al.*, 1995, 1998] which used a combinatorial approach, can be recovered in this investigation.

In the following discussions, the symbols "+" and "−", if not in an arithmetic computation, are used to represent the positive and negative saturated states as well as their output patterns, respectively. Thus, the elements in the set $\mathcal{A}^{T_n}$, $\mathcal{A} = \{+, -\}$, give all possible mosaic patterns on T_n.

This presentation is organized as follows. In Sec. 2, the relation between the existence of basic patterns and the parameters is discussed. The parameter space is then partitioned into finitely many regions for the illustrative case, that is, for the

1×3 template. The basic patterns that exist for the parameters in each partitioned region will then be identified. The formulations of transition matrices and boundary-pattern matrices are presented in Sec. 3. The computations on the number of mosaic patterns are then summarized. In Sec. 4, we extend the above formulations to CNN with 1×5 template.

2. Partition of the Parameter Space

We shall first present the fundamental ideas of basic patterns for general one-dimensional template. Associated with the notion of basic pattern, a partitioning of the parameter space can be performed so that basic patterns can be determined for each parameter region. We shall illustrate the partitioning for the 1×3 template.

Consider the general one-dimensional template,

$$A_r = [\beta_{-r} \cdots \beta_{-1} \quad a \quad \beta_1 \cdots \beta_r]\,.$$

For each positive integer ℓ, set

$$Y_\ell = \{y = (y_1, y_2, \ldots, y_\ell)\,, \quad y_i = 1, \text{ or } -1\}\,.$$

Let y be an element of Y_n. Then, on the one hand, y is a mosaic pattern on T_n if and only if for each $i \in I[1, n]$,

$$\sum_{1\le|k|\le r} \beta_k y_{i+k} + a + z > 1 \qquad \text{if } y_i = 1\,, \tag{2}$$

$$\sum_{1\le|k|\le r} \beta_k y_{i+k} - a + z < -1 \qquad \text{if } y_i = -1\,. \tag{3}$$

Herein, y_{i+k}, $i + k \notin T_n$, are determined from the imposed B.C. On the other hand, let $\hat{y} = (y_{m-r}, \ldots, y_{m-1}, y_m, y_{m+1}, \ldots, y_{m+r}) \in Y_{2r+1}$, which satisfies (2) or (3) for $i = m$, then there exists $(x_{m-r}, \ldots, x_{m-1}, x_m, x_{m+1}, \ldots, x_{m+r}) \in \mathbf{R}^{2r+1}$, with $f(x_i) = y_i$, which satisfies (1) for $i = m$. Let $\tilde{y} = (y_{m-r+1}, \ldots, y_{m-1}, y_m, y_{m+1}, \ldots, y_{m+r}, y_{m+r+1})$ be another element in Y_{2r+1}, which satisfies (2) or (3) for $i = m + 1$. Then attaching $\tilde{y}$ to the right of $\hat{y}$ with the $2r$ coinciding components overlapped, one obtains a pattern $(y_{m-r}, \ldots, y_{m-1}, y_m, y_{m+1}, \ldots, y_{m+r}, y_{m+r+1})$ which is of size $2r+2$. There corresponds a $(2r+2)$-tuple $(x_{m-r}, \ldots, x_{m-1}, x_m, x_{m+1}, \ldots, x_{m+r}, x_{m+r+1})$ which satisfies the stationary equation of (1) with $i = m, m + 1$. This is the motivation for introducing the basic patterns. Accordingly, the set of basic patterns corresponding to the template A_r and the bias z is defined as

$$\mathcal{B}(A_r, z) := \mathcal{B}^+(A_r, z) \cup \mathcal{B}^-(A_r, z)\,,$$

where

$$\mathcal{B}^+(A_r, z) = \Bigg\{ y \in Y_{2r+1} : y_{r+1} = 1, \sum_{1\le|k|\le r} \beta_k y_{r+k+1} + a + z - 1 > 0 \Bigg\}\,,$$

$$\mathcal{B}^-(A_r, z) = \Bigg\{ y \in Y_{2r+1} : y_{r+1} = -1, \sum_{1\le|k|\le r} \beta_k y_{r+k+1} - a + z + 1 < 0 \Bigg\}\,.$$

These are the basic patterns with "$+$" in the center and with "$-$" in the center, respectively. The following notion of total-output corresponding to the template A_r has been introduced in [Shih, 1998] and [Juang & Lin, 2000]. We shall use this notion to describe the existence of basic patterns.

Definition 2.1. Let $(x_1, x_2, \ldots, x_n)$ be a stationary solution of (1) with template A_r, the total-output for the cell C_i at the site i is defined by

$$TO(i) = \sum_{1\le|k|\le r} \beta_k f(x_{i+k}) = \sum_{1\le|k|\le r} \beta_k y_{i+k}\,.$$

To construct mosaic patterns on T_n with given parameters, one needs to determine the elements in $\mathcal{B}(A_r, z)$. On the other hand, there are different sets of parameters (A_r, z) for which the corresponding basic patterns $\mathcal{B}(A_r, z)$ are identical. In fact, the parameter space $\{z, a, \beta_i : |i| \in I[1, r]\}$ can be decomposed into finitely many regions such that basic patterns for (1) with the parameters in the same region are identical. Such a partitioning has been explored in [Juang & Lin, 2000] for one-dimensional and two-dimensional CNN with symmetric templates and in [Hsu *et al.*, 2000] for general templates. Herein, we recall the partitioning for the one-dimensional CNN with template $A_1 = [\beta_{-1} \quad a \quad \beta_1]$, that is, $r = 1$, cf. [Shih, 2000].

In the following discussions, we represent $y_i = 1$ or -1, the output at the cell C_i, by $y_i =$ "$+$" or "$-$" respectively. There are at most eight basic patterns, namely, $\overline{+++}$, $\overline{++-}$, $\overline{-++}$, $\overline{-+-}$, $\overline{---}$, $\overline{--+}$, $\overline{+--}$, $\overline{+-+}$, corresponding to template A_1 with $\beta_{-1}, \beta_1 \neq 0$. We collect them into two groups,

$$\tilde{\mathcal{B}}^+ = \{\overline{\mathrm{w}+\mathrm{e}}\,|\,\mathrm{w}, \mathrm{e} = \text{"}+\text{" or "}-\text{"}\} \tag{4}$$

$$\tilde{\mathcal{B}}^{-} = \{\overline{\mathrm{w}-\mathrm{e}}\,|\mathrm{w},\, \mathrm{e} = \text{“}+\text{”} \text{ or } \text{“}-\text{”}\}\,. \qquad (5)$$

Herein, the notation “w” represents west, while “e” denotes east. Assume that the basic patterns are situated at the sites $\{i-1, i, i+1\}$. Accordingly, we define the total-output $TO(+)$ (resp. $TO(-)$) for the basic pattern $\overline{\mathrm{w}+\mathrm{e}}$ (resp. $\overline{\mathrm{w}-\mathrm{e}}$) as the total-output of the central cell of these 1×3 patterns. Restated, $TO(+)$ or $TO(-) = TO(i) = \beta_{-1}\sigma_{\mathrm{w}} + \beta_1\sigma_{\mathrm{e}}$, where $\sigma_{\mathrm{w}} = 1, -1$ if w = “+”, “−” respectively, and $\sigma_{\mathrm{e}} = 1, -1$ if e = “+”, “−” respectively. We shall order the elements in $\tilde{\mathcal{B}}^{+}$ (resp. $\tilde{\mathcal{B}}^{-}$) according to the decreasing (resp. increasing) values of their total-outputs. For example, assume that (β_{-1}, β_1) is in the range $\beta_{-1} > \beta_1 > 0$. Then the elements of $\tilde{\mathcal{B}}^{+}$ are ordered, from the first to the last, as $\overline{+++}$, $\overline{++-}$, $\overline{-++}$, $\overline{-+-}$, since the total-outputs of these basic patterns are, respectively, $\beta_{-1}+\beta_1$, $\beta_{-1}-\beta_1$, $\beta_1-\beta_{-1}$, $-\beta_{-1}-\beta_1$, which are in an order of decreasing values. In addition, the elements of $\tilde{\mathcal{B}}^{-}$ are ordered, from the first to the last, as $\overline{---}$, $\overline{--+}$, $\overline{+--}$, $\overline{+-+}$, since the total-outputs of these patterns are respectively, $-\beta_{-1}-\beta_1$, $\beta_1-\beta_{-1}$, $\beta_{-1}-\beta_1$, $\beta_{-1}+\beta_1$, which are in an order of increasing values. Notably, this ordering depends on the location of (β_{-1}, β_1) in the partitioned regions in Fig. 1.

The notations in Fig. 2 are interpreted as follows. For $m, n \in I[0, 4]$, $(z, a) \in [m, n]$ means that $\mathcal{B}^{+}(A_1, z)$ consists of the first m elements in $\tilde{\mathcal{B}}^{+}$ and $\mathcal{B}^{-}(A_1, z)$ consists of the first n elements in $\tilde{\mathcal{B}}^{-}$. Notice that the orders of the elements in $\tilde{\mathcal{B}}^{+}$ and $\tilde{\mathcal{B}}^{-}$ are dependent on the location of (β_{-1}, β_1) in the partitioned regions in Fig. 1. The equations of the lines in Fig. 2 are given by $\ell_k^{+} : a+z = 1+c_k^{+}$, $\ell_k^{-} : a-z = 1+c_k^{-}$, where c_k^{+} (resp. c_k^{-}) is the total-

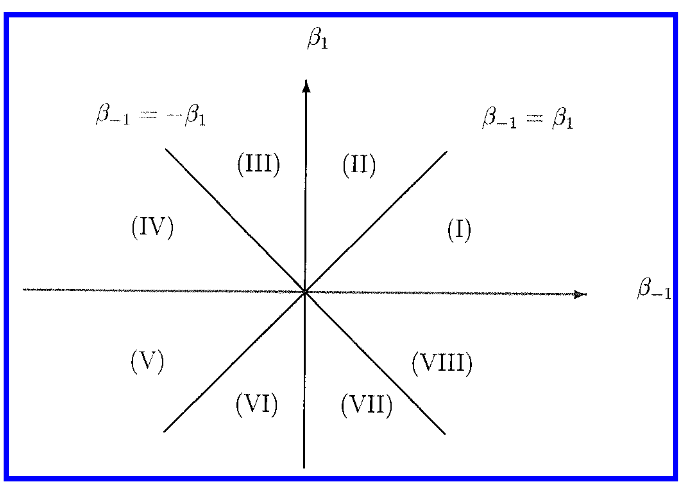

Fig. 1. Primary partition of (β_{-1}, β_1)-plane.

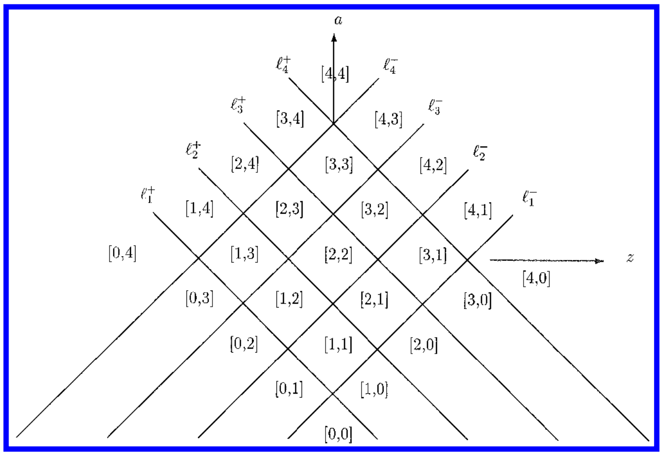

Fig. 2. Partition of (z, a)-plane for given $\beta_{-1} \neq 0$, $\beta_1 \neq 0$, $\beta_{-1} \neq \pm\beta_1$.

output of the $(5-k)$-th elements in $\tilde{\mathcal{B}}^{+}$ (resp. the kth element in $\tilde{\mathcal{B}}^{-}$).

If the zero Dirichlet boundary condition (D_0-B.C.) is considered, the patterns $\overline{+\mathrm{e}}$, or $\overline{-\mathrm{e}}$, e = “+” or “−”, at the sites $\{1, 2\}$ and $\overline{\mathrm{w}+}$, or $\overline{\mathrm{w}-}$, w = “+” or “−”, at the sites $\{n-1, n\}$ will be bordered by zero, the prescribed data. Hence, the following patterns need to be considered,

$$0|\overline{++}\,,\ 0|\overline{+-}\,,\ \overline{++}|0\,,\ \overline{-+}|0\,,$$
$$0|\overline{--}\,,\ 0|\overline{-+}\,,\ \overline{+-}|0\,,\ \overline{--}|0\,.$$

We define the total-output for each of these 1×3 patterns as the total-output for the “+” or “−” at its central site. The latter one is given by Definition 2.1. These 1×3 patterns may now be ordered according to their total-outputs. Let

$$\tilde{\mathcal{B}}_0^{+} = \{0|\overline{+\mathrm{e}},\ \overline{\mathrm{w}+}|0 : \mathrm{w},\, \mathrm{e} = \text{“}+\text{”} \text{ or } \text{“}-\text{”}\} \qquad (6)$$
$$\tilde{\mathcal{B}}_0^{-} = \{0|\overline{-\mathrm{e}},\ \overline{\mathrm{w}-}|0 : \mathrm{w},\, \mathrm{e} = \text{“}+\text{”} \text{ or } \text{“}-\text{”}\}\,. \qquad (7)$$

The elements in $\tilde{\mathcal{B}}_0^{+}$ (resp. $\tilde{\mathcal{B}}_0^{-}$) will be ordered according to the decreasing (resp. increasing) values of their total-outputs. Let us take the parameters (β_{-1}, β_1) in the region $\beta_{-1} > \beta_1 > 0$ for an illustration. The elements of $\tilde{\mathcal{B}}_0^{+}$ are ordered, from the first to the last, as $\overline{++}|0$, $0|\overline{++}$, $0|\overline{+-}$, $\overline{-+}|0$, since the total-outputs of these basic patterns are, respectively, β_{-1}, β_1, $-\beta_1$, $-\beta_{-1}$. Moreover, the elements of $\tilde{\mathcal{B}}_0^{-}$ are ordered, from the first to the last, as $\overline{--}|0$, $0|\overline{--}$, $0|\overline{-+}$, $\overline{+-}|0$, since the total-outputs of these patterns are respectively, $-\beta_{-1}$, $-\beta_1$, β_1, β_{-1}.

For the D_0-B.C., to classify the existence of the boundary patterns in (6), (7) with respect to

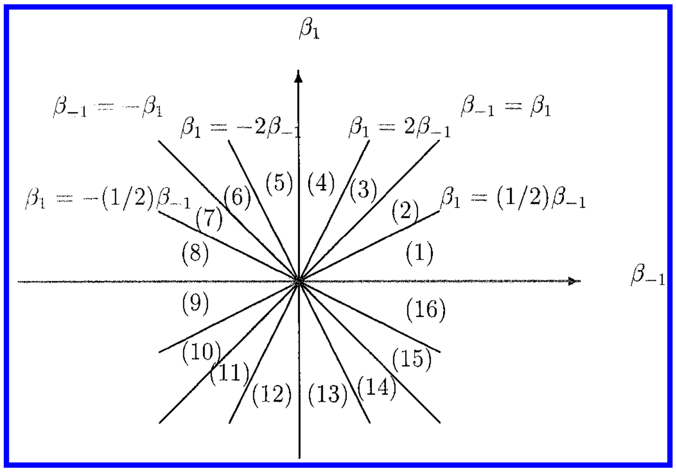

Fig. 3. Further partition of (β_{-1}, β_1)-plane for the D_0 boundary condition.

parameters, the parameter space requires further partitioning. Firstly, the (β_{-1}, β_1)-plane is partitioned, as shown in Fig. 3, to determine the ordering for total-outputs of the elements in $\tilde{\mathcal{B}}^+ \cup \tilde{\mathcal{B}}_0^+$ and the ones in $\tilde{\mathcal{B}}^- \cup \tilde{\mathcal{B}}_0^-$. Consequently, for (β_{-1}, β_1) in each of the regions in Fig. 3, the set of feasible basic patterns, $\mathcal{B}(A_1, z)$, and the set of feasible boundary patterns, $\mathcal{B}_0(A_1, z) = \mathcal{B}_0^+(A_1, z) \cup \mathcal{B}_0^-(A_1, z)$, can be determined and classified with respect to the parameters (z, a). Accordingly, finer partitioning is performed for the (z, a)-plane, as shown in Fig. 4. The equations of these new separating lines in Fig. 4 are given by $\ell_{0,k}^+ : a + z = 1 + c_{0,k}^+$, $\ell_{0,k}^- : a - z = 1 + c_{0,k}^-$, where $c_{0,k}^+$, $c_{0,k}^-$ are the total-outputs of the $(5-k)$-th and the kth elements of $\tilde{\mathcal{B}}_0^+$ and $\tilde{\mathcal{B}}_0^-$ respectively. The feasible boundary patterns (the elements of $\mathcal{B}_0(A_1, z)$) for parameters in

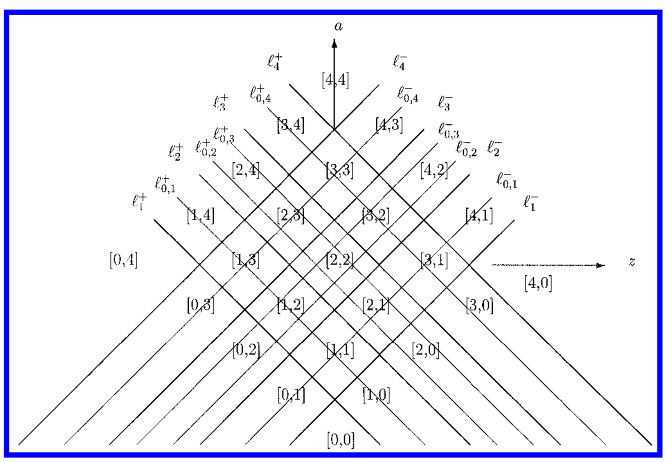

Fig. 4. Further partition of (z, a)-plane for the D_0 boundary condition, given $\beta_{-1} \neq 0$, $\beta_1 \neq 0$, $\beta_{-1} \neq \pm\beta_1$.

each partitioned region in Fig. 4 are described as follows. If (z, a) lies in the region above $\ell_{0,m}^+$ and $\ell_{0,k}^-$, $m, k \in I[1, 4]$, for the largest possible m, k, then $\mathcal{B}_0^+(A_1, z)$ consists of the first m elements in (6) and $\mathcal{B}_0^-(A_1, z)$ consists of the first k elements in (7).

3. Boundary-Pattern and Transition Matrices

Assume that z and the parameters in the 1×3 template $A_1 = [\beta_{-1} \quad a \quad \beta_1]$ are given. The set of basic patterns $\mathcal{B}(A_1, z)$ for (1) with these parameters can then be determined as in Sec. 2. Taking the following identifications between the indices and the four 1×2 patterns:

$$1 \leftrightarrow ++, \quad 2 \leftrightarrow +-, \quad 3 \leftrightarrow -+, \quad 4 \leftrightarrow --, \tag{8}$$

we consider the transition matrix M,

$$M = \begin{bmatrix} m_{11} & m_{12} & 0 & 0 \\ 0 & 0 & m_{23} & m_{24} \\ m_{31} & m_{32} & 0 & 0 \\ 0 & 0 & m_{43} & m_{44} \end{bmatrix}, \tag{9}$$

where $m_{ij} = 0$ or 1. The formation of basic patterns can be described as follows: the (i, j)-entry of M is one if and only if the jth 1×2 pattern in (8) can be joined, with one site overlapped, to the right of the ith 1×2 pattern in (8) to form a 1×3 basic pattern in $\mathcal{B}(A_1, z)$.

The transition matrix thus formulated can be used to generate patterns on lattices of larger size (of length greater than three). For example, the (1, 2)-entry of M^2, which is in fact $m_{11}m_{12}$, gives the number of patterns $(y_k, y_{k+1}, y_{k+2}, y_{k+3}) = (+, +, +, -)$ on a 1×4 lattice (let us take $k+1$, $k+2 \in T_n \backslash \mathbf{b}$). The existence of this pattern indicates that there exists $(x_k, x_{k+1}, x_{k+2}, x_{k+3}) \in \mathbf{R}^4$ with x_k, x_{k+1}, $x_{k+2} > 1$ and $x_{k+3} < -1$ such that the stationary equation of (1) is satisfied for $i = k+1, k+2$. Subsequently, it can be deduced that the sum of entries of M^{n-2} gives the number of patterns on T_n. Each of these patterns $y = (y_1, y_2, \ldots, y_{n-1}, y_n)$ ensures the existence of $x = (x_1, x_2, \ldots, x_{n-1}, x_n) \in \mathbf{R}^n$ with $x_i > 1$ if $y_i =$ "+" and $x_i < -1$ if $y_i =$ "−". Moreover, x satisfies the stationary equation of (1) for $i \in I[2, n-1]$. To determine if y (resp. x) is indeed a mosaic pattern (resp. mosaic solution) on T_n, it suffices to check if y_1, y_2 and y_{n-1}, y_n match the boundary condition.

This task can be resolved by observing further property of the transition matrices. Indeed, the (i, j)-entry of M^{n-2} gives the number of patterns on T_n with the ith 1×2 pattern in (8) at the two sites to the far left of T_n and the jth 1×2 pattern in (8) at the two sites to the far right of T_n. For instance, the (2, 4)-entry of M^{n-2} gives the number of patterns on T_n with the left-hand side having "$+-$" and the right-hand side having "$--$", that is, patterns of the following form,

$$\boxed{+-\cdots\cdots\cdots\cdots--}\,. \tag{10}$$

This information and our formulation of basic patterns allow us to count the number of mosaic patterns on T_n with any boundary condition mentioned in Sec. 1. We shall describe the feasible patterns on the boundary sites with respect to the imposed B.C. also by a matrix, called *boundary-pattern matrix*. Let us describe these matrices M_{N}, M_{P}, M_{D} corresponding to the Neumann, periodic, and Dirichlet boundary condition respectively. Set

$$M_{\mathrm{B}} = \begin{bmatrix} b_{11} & b_{12} & b_{13} & b_{14} \\ b_{21} & b_{22} & b_{23} & b_{24} \\ b_{31} & b_{32} & b_{33} & b_{34} \\ b_{41} & b_{42} & b_{43} & b_{44} \end{bmatrix}, \tag{11}$$

where B = N, P, D_1, D_0. We take (10) as an example to explain the construction of M_{B}. That is, we consider the following situation:

$$\mathrm{w}\boxed{+-\cdots\cdots\cdots\cdots--}\mathrm{e}\,. \tag{12}$$

If B = N, for the pattern in (10) to satisfy the Neumann B.C., w and e in (12) have to be w = "+", e = " $-$ ". That is, $\overline{\underline{++-}}$ and $\overline{\underline{---}}$ have to be feasible basic patterns (elements of $\mathcal{B}(A_1, z)$). If this is the case, then $(M_{\mathrm{N}})_{24} = b_{24} = 1$, otherwise, $(M_{\mathrm{N}})_{24} = b_{24} = 0$. For the pattern in (10) to satisfy the periodic B.C., w and e in (12) have to be w $= y_n$, e $= y_1$, that is, w = " $-$ ", e = "+". Thus, if $\overline{\underline{-+-}}$ and $\overline{\underline{--+}}$ are feasible, then $(M_{\mathrm{P}})_{24} = b_{24} = 1$, otherwise, $(M_{\mathrm{P}})_{24} = b_{24} = 0$. If B = D_1, that is, the Dirichlet B.C. with saturated prescribed data, similar results can be derived. The entries of M_{B} can thus be obtained as follows. If B = N,

$$\begin{array}{lll} b_{11} = m_{11}^2 & b_{12} = m_{11}m_{24} & b_{13} = m_{11}m_{31} \\ b_{14} = m_{11}m_{44} & b_{21} = m_{12}m_{11} & b_{22} = m_{12}m_{24} \\ b_{23} = m_{12}m_{31} & b_{24} = m_{12}m_{44} & b_{31} = m_{43}m_{11} \\ b_{32} = m_{43}m_{24} & b_{33} = m_{43}m_{31} & b_{34} = m_{43}m_{44} \\ b_{41} = m_{44}m_{11} & b_{42} = m_{44}m_{24} & b_{43} = m_{44}m_{31} \\ b_{44} = m_{44}^2\,. & & \end{array} \tag{13}$$

If B = P,

$$\begin{array}{lll} b_{11} = m_{11}^2 & b_{12} = m_{23}m_{31} & b_{13} = m_{31}m_{11} \\ b_{14} = m_{43}m_{31} & b_{21} = m_{11}m_{12} & b_{22} = m_{23}m_{32} \\ b_{23} = m_{31}m_{12} & b_{24} = m_{43}m_{32} & b_{31} = m_{12}m_{23} \\ b_{32} = m_{24}m_{43} & b_{33} = m_{32}m_{23} & b_{34} = m_{44}m_{43} \\ b_{41} = m_{12}m_{24} & b_{42} = m_{24}m_{44} & b_{43} = m_{32}m_{24} \\ b_{44} = m_{44}^2\,. & & \end{array} \tag{14}$$

In fact, $(M_{\mathrm{P}})_{ij} = (M^2)_{ji}$. If B = D_1 with $\tilde{y}_0 = \tilde{y}_{n+1} =$ " + ", then

$$\begin{array}{lll} b_{11} = m_{11}^2 & b_{12} = m_{11}m_{23} & b_{13} = m_{11}m_{31} \\ b_{14} = m_{11}m_{43} & b_{21} = m_{12}m_{11} & b_{22} = m_{12}m_{23} \\ b_{23} = m_{12}m_{31} & b_{24} = m_{12}m_{43} & b_{31} = m_{23}m_{11} \\ b_{32} = m_{23}m_{23} & b_{33} = m_{23}m_{31} & b_{34} = m_{23}m_{43} \\ b_{41} = m_{24}m_{11} & b_{42} = m_{24}m_{23} & b_{43} = m_{24}m_{31} \\ b_{44} = m_{24}m_{43}\,. & & \end{array} \tag{15}$$

If B = D_0, then $\mathcal{B}_0(A_1, z)$ consists of the 1×2 patterns in (8) which can be bordered by 0 from the left or from the right. Accordingly, $(M_{\mathrm{D}_0})_{ij} = 1$ if and only if the ith pattern in (8) can be bordered by 0 from the left and the jth pattern in (8) can be bordered by 0 from the right. For example, $(M_{\mathrm{D}_0})_{23} = 1$ if and only if (16) is feasible.

$$0|\overline{\underline{+-}},\ \overline{\underline{-+}}|0\,. \tag{16}$$

The following main theorem of this presentation focuses on CNN with the above-discussed 1×3 template. Extension to more general one-dimensional templates follows from suitable formulations on the corresponding transition matrix and boundary-pattern matrix. The case of the 1×5 template will be sketched in the next section.

Theorem 3.1. *Consider CNN on T_n with template $A_1 = [\beta_{-1}\quad a\quad \beta_1]$. The total number of* *mosaic patterns on* T_n *satisfying boundary condition* B, B $=$ P, N, D_1, D_0 *is given by*

$$\sum_{i,j=1}^{4} (M_{\mathrm{B}})_{ij}(M^{n-2})_{ij}\,, \tag{17}$$

where M, M_{B} *are as described in* (*9*), (*11*), (*13*)–(*15*).

As an illustration, exact numbers of moasic patterns resulting from computations of (17) for some parameter regions of Figs. 1–4 are presented in the following tables. Table 1 concerns itself with the Neumann and periodic boundary conditions for parameters in regions of Figs. 1 and 2. Table 2 is concerned with the zero Dirichlet boundary condition for parameters in regions of Figs. 3 and 4. In the tables, $\Gamma_1(n) = [(1+\sqrt{5}/2)^n + (1-\sqrt{5}/2)^n] + 2\cos[(2\pi/3)n]$, $\Gamma_2(n) = (2/\sqrt{5})[(1+\sqrt{5}/2)^{n+1} - (1-\sqrt{5}/2)^{n+1}]$. In Table 2, $[3, 3]_1$ (resp. $[3, 3]_2$) represents the subregion of $[3, 3]$, which lies above (resp. below) $\ell^+_{0,4}$ and $\ell^-_{0,4}$, while $[2, 2]_1$ represents the subregion of $[2, 2]$, which lies above $\ell^+_{0,3}$ and $\ell^-_{0,3}$. Note that there is a symmetry between the feasible patterns and the corresponding parameter regions, cf. [Shih, 1998]. The symmetry results in identical number of patterns for some parameter regions, as shown in the first columns of the tables.

We shall only illustrate the computations for three cases, one for each type of boundary condition.

Table 1. Exact number of mosaic patterns for CNN with the Neumann and periodic boundary conditions.

Region in (β_{-1}, β_1)-plane	Regions in (z, a)-plane	Neumann	Periodic
(I), (II)	[4, 4]	2^n	2^n
	[3, 3]	$\Gamma_2(n)$	$\Gamma_1(n)$
	[2, 2]	2	2
(III), (VIII)	[4, 4]	2^n	2^n
	[3, 3]	2	$3+(-1)^n$
	[2, 2]	0	2
(IV), (VII)	[4, 4]	2^n	2^n
	[3, 3]	2	$3+(-1)^n$
	[2, 2]	0	$1+(-1)^n$
(V), (VI)	[4, 4]	2^n	2^n
	[3, 3]	$\Gamma_2(n)$	$\Gamma_1(n)$
	[2, 2]	2	$1+(-1)^n$

Table 2. Exact number of mosaic patterns for CNN with the zero Dirichlet boundary condition.

Region in (β_{-1}, β_1)-plane	Regions in (z, a)-plane	Dirichlet D_0
(1), (4)	[4, 4]	2^n
	$[3, 3]_1$	$\Gamma_2(n+1)$
	$[3, 3]_2$	2
	$[2, 2]_1$	2
(2), (3)	[4, 4]	2^n
	$[3, 3]_1$	$\Gamma_2(n+1)$
	$[3, 3]_2$	$\Gamma_2(n)$
	$[2, 2]_1$	$\Gamma_2(n-1)$
(5), (16)	[4, 4]	2^n
	$[3, 3]_1$	$2n$
	$[3, 3]_2$	2
	$[2, 2]_1$	0
(6), (15)	[4, 4]	2^n
	$[3, 3]_1$	$2n$
	$[3, 3]_2$	0
	$[2, 2]_1$	0
(7), (14)	[4, 4]	2^n
	$[3, 3]_1$	$2n$
	$[3, 3]_2$	0
	$[2, 2]_1$	0
(8), (13)	[4, 4]	2^n
	$[3, 3]_1$	$2n$
	$[3, 3]_2$	2
	$[2, 2]_1$	0

(i) Consider (β_{-1}, β_1) in the region (I) of Fig. 1 and (z, a) in the region $[3, 3]$ of Fig. 2. The corresponding feasible basic patterns are

$$\mathcal{B}^+(A_1, z) = \{\overline{\underline{+++}},\ \overline{\underline{++-}},\ \overline{\underline{-++}}\}$$
$$\mathcal{B}^-(A_1, z) = \{\overline{\underline{---}},\ \overline{\underline{--+}},\ \overline{\underline{+--}}\}\,.$$

It follows that the entries of the transition matrix (9) are $m_{11} = m_{12} = m_{24} = m_{31} = m_{43} = m_{44} = 1$, and $m_{ij} = 0$ for the other $i, j \in I[1, 4]$. Herein, we only demonstrate the case of Neumann boundary condition. In this case, every entry of M_{N} is one, as computed from (13). Therefore, the total number of mosaic patterns on T_n satisfying the Neumann boundary condition can be computed by (17). It can be calculated, with help from symbolic computation of Mathematica software, that

$$\sum_{i,j=1}^{4}(M_{\mathrm{N}})_{ij}(M^{n-2})_{ij}=\frac{2}{\sqrt{5}}\left[\left(\frac{1+\sqrt{5}}{2}\right)^{n+1}-\left(\frac{1-\sqrt{5}}{2}\right)^{n+1}\right].$$

(ii) Consider $(\beta_{-1},\, \beta_1)$ in the region (III) of Fig. 1 and $(z,\, a)$ in the region $[3, 3]$ of Fig. 2. The corresponding feasible basic patterns are

$$\mathcal{B}^{+}(A_1,\, z)=\{\overline{-++},\ \overline{+++},\ \overline{-+-}\} \tag{18}$$

$$\mathcal{B}^{-}(A_1,\, z)=\{\overline{+--},\ \overline{---},\ \overline{+-+}\}. \tag{19}$$

Consequently, the entries of the transition matrix (9) are $m_{11}=m_{23}=m_{24}=m_{31}=m_{32}=m_{44}=1$, and $m_{ij}=0$ for the other $i,\, j\in I[1,\, 4]$. Herein, we consider the case of a periodic boundary condition. Following the formula in (14), the entries of M_{P} are $b_{11}=b_{12}=b_{13}=b_{22}=b_{33}=b_{42}=b_{43}=b_{44}=1$, and $b_{ij}=0$ for the other $i,\, j\in I[1,\, 4]$. There are many patterns for the interior cells. However, imposing the periodic boundary condition strongly limits the number of feasible patterns on T_n. The total number of mosaic patterns on T_n satisfying the periodic boundary condition is computed as

$$\sum_{i,j=1}^{4}(M_{\mathrm{P}})_{ij}(M^{n-2})_{ij}=3+(-1)^n.$$

(iii) Consider $(\beta_{-1},\, \beta_1)$ in the region (6) of Fig. 3 and $(z,\, a)$ in the region $[3,\, 3]_1$ of Fig. 4. The corresponding feasible basic patterns are the same as (18) and (19). Therefore, the entries of the transition matrix (9) are $m_{11}=m_{23}=m_{24}=m_{31}=m_{32}=m_{44}=1$, and $m_{ij}=0$ for the other $i,\, j\in I[1,\, 4]$. Herein, we consider the case of zero Dirichlet boundary condition. The following boundary patterns are feasible,

$$\tilde{\mathcal{B}}_0^{+}(A_1,\, z)=\{0|\overline{++},\ \overline{++}|0,\ \overline{-+}|0\}$$

$$\tilde{\mathcal{B}}_0^{-}(A_1,\, z)=\{0|\overline{-+},\ \overline{--}|0,\ \overline{+-}|0\}.$$

As a consequence, the entries of M_{D_0} are $b_{1j}=1$, $b_{4j}=1$, $j\in I[1,\, 4]$, and $b_{ij}=0$ for the other $i,\, j\in I[1,\, 4]$. The total number of mosaic patterns on T_n satisfying the zero Dirichlet boundary condition is thus

$$\sum_{i,j=1}^{4}(M_{\mathrm{D}_0})_{ij}(M^{n-2})_{ij}=2n.$$

4. Formulation for 1 × 5 Template

In this section, we shall extend the formulations of transition matrix and boundary-pattern matrix to CNN with 1×5 template. Namely, we consider $r=2$ and the template

$$A_2=[\beta_{-2}\quad \beta_{-1}\quad a\quad \beta_1\quad \beta_2].$$

Herein, the partitioning for the $(\beta_{-2},\, \beta_{-1},\, \beta_1,\, \beta_2)$-space is performed so that sixteen possible total-outputs $\beta_{-2}\pm\beta_{-1}\pm\beta_1\pm\beta_2$ for a cell can be ordered in each partitioned parameter region. With given β_{-2}, β_{-1}, β_1, β_2, the $(z,\, a)$-plane can be partitioned so that the existence of basic patterns can be determined for each parameter region of $(z,\, a)$-plane.

There are 32 possible basic patterns corresponding to template A_2; namely, $\overline{\bullet\bullet\bullet\bullet\bullet}$, where $\bullet$ = " + " or " − ". A 16×16 transition matrix $M=[m_{ij}]$ can be formulated to produce mosaic patterns on T_n from basic patterns. We take the following identifications between the indices of the matrix M and the sixteen 1×4 patterns:

$$\begin{array}{lll} 1\leftrightarrow ++++\,, & 2\leftrightarrow +++-\,, & 3\leftrightarrow ++-+\,,\\ 4\leftrightarrow ++--\,, & 5\leftrightarrow +-++\,, & 6\leftrightarrow +-+-\,,\\ 7\leftrightarrow +--+\,, & 8\leftrightarrow +---\,, & 9\leftrightarrow -+++\,,\\ 10\leftrightarrow -++-\,, & 11\leftrightarrow -+-+\,, & 12\leftrightarrow -+--\,,\\ 13\leftrightarrow --++\,, & 14\leftrightarrow --+-\,, & 15\leftrightarrow ---+\,,\\ 16\leftrightarrow ----\,. & & \end{array} \tag{20}$$

In the matrix M, the entries $m_{ij}=0$ or 1 for $i\in I[1,\, 8]$, $j=(i+i-1)$, $(i+i)$, and for $i\in I[9,\, 16]$, $j=(2i-18+1)$, $(2i-18+2)$. All other entries are set to zero. The possible nonzero entries are defined as follows: $m_{ij}=1$ if and only if attaching the jth 1×4 pattern in (20), with three sites overlapped, to the right of the ith 1×4 pattern in (20) constitutes a feasible 1×5 basic pattern. Notably, the purpose of overlapping three sites in the attaching process is to guarantee the feasibility of produced patterns.

The boundary-pattern matrix $M_{\mathrm{B}}=[b_{ij}]$ is also a 16×16 matrix. For example, consider periodic boundary condition and the following enclosed pattern on T_n,

$$\mathrm{w}_2\mathrm{w}_1\boxed{++++\cdots\cdots\cdots+++-}\,\mathrm{e}_1\mathrm{e}_2\,. \tag{21}$$

In (21), four "+" at the left end corresponds to the first pattern in (20) and "+ + +−" at the right end corresponds to the second pattern in (20). According to analogous setting in Sec. 3, $b_{12} = 1$ if and only if $\mathrm{w}_2 = \text{“}+\text{”} = y_{n-1}$, $\mathrm{w}_1 = \text{“}-\text{”} = y_n$ and $\mathrm{e}_1 = \text{“}+\text{”} = y_1$, $\mathrm{e}_2 = \text{“}+\text{”} = y_2$ are allowed as the neighbors for the cells at $\{1, 2\}$ and $\{n-1, n\}$ in (21). More precisely, $b_{12} = m_{59}m_{91}m_{23}m_{35}$. The detailed formulation is rather straightforward and is omitted. A formula similar to (17) can thus be derived for CNN with template A_2.

References

Chow, S. N. & Mallet-Paret, J. [1995] "Pattern formation and spatial chaos in lattice dynamical system I," *IEEE Trans. Circuits Syst.* **42**, 746–751.

Chow, S. N., Mallet-Paret, J. & Van Vleck, E. S. [1996] "Pattern formation and spatial chaos in spatially discrete evolution equations," *Rand. Comput. Dyn.* **4**, 109–178.

Chua, L. O. & Yang, L. [1988a] "Cellular neural networks: Theory," *IEEE Trans. Circuits Syst.* **35**, 1257–1272.

Chua, L. O. & Yang, L. [1988b] "Cellular neural networks: Applications," *IEEE Trans. Circuits Syst.* **35**, 1273–1290.

Chua, L. O. [1998] *CNN: A Paradigm for Complexity*, World Scientific Series on Nonlinear Science, Series A, Vol. 31 (World Scientific, Singapore).

Hsu, C. H., Juang, J., Lin, S. S. & Lin, W. W. [2000] "Cellular neural network: Local patterns for general template," *Int. J. Bifurcation and Chaos* **10**(7), 1645–1659.

Juang, J. & Lin, S. S. [1997] "Cellular neural networks II: Defect pattern and spatial chaos," preprint.

Juang, J. & Lin, S. S. [2000] "Cellular neural networks I: Mosaic pattern and spatial chaos," *SIAM J. Appl. Math* **60**(3), 891–915.

Lin, S. S. & Shih, C. W. [1999] "Complete stability for standard cellular neural networks," *Int. J. Bifurcation and Chaos* **9**(5), 909–918.

Lin, S. S. & Yang, C. S. [2000] "Spatial entropy of 1-dimensional cellular neural network," *Int. J. Bifurcation and Chaos* **10**(9), 2129–2141.

Robinson, C. [1995] *Dynamical Systems* (CRC Press, Boca Raton, FL).

Shih, C. W. [1998] "Pattern formation and spatial chaos for cellular neural network with asymmetric templates," *Int. J. Bifurcation and Chaos* **8**(10), 1907–1936.

Shih, C. W. [2000] "Influence of boundary conditions on pattern formation and spatial chaos for lattice systems," *SIAM J. Appl. Math.* **61**(1), 335–368.

Thiran, P. [1993] "Influence of boundary conditions on the behavior of cellular neural networks," *IEEE Trans. Circuits Syst. I: Fundamental Th. Appl.* **40**(3), 207–212.

Thiran, P., Crounse, K. R., Chua, L. O. & Hasler, M. [1995] "Pattern formation properties of autonomous cellular neural networks," *IEEE Trans. Circuit Syst.* **42**, 757–774.

Thiran, P., Setti, G. & Hasler, M. [1998] "An approach to information propagation in 1-D cellular nueral network — Part I: Local diffusion," *IEEE Trans. Circuit Syst.* **45**, 777–789.

This article has been cited by:

1. Jung-Chao Ban. 2014. Neural network equations and symbolic dynamics. *International Journal of Machine Learning and Cybernetics* . [CrossRef]
2. Jung-Chao Ban, Chih-Hung Chang. 2013. Inhomogeneous lattice dynamical systems and the boundary effect. *Boundary Value Problems* **2013**:1, 249. [CrossRef]
3. WEN-GUEI HU, SONG-SUN LIN. 2009. ZETA FUNCTIONS FOR HIGHER-DIMENSIONAL SHIFTS OF FINITE TYPE. *International Journal of Bifurcation and Chaos* **19**:11, 3671-3689. [Abstract] [References] [PDF] [PDF Plus]
4. JUNG-CHAO BAN, CHIH-HUNG CHANG. 2008. ON THE DENSE ENTROPY OF TWO-DIMENSIONAL INHOMOGENEOUS CELLULAR NEURAL NETWORKS. *International Journal of Bifurcation and Chaos* **18**:11, 3221-3231. [Abstract] [References] [PDF] [PDF Plus]
5. SONG-SUN LIN, WEN-WEI LIN, TING-HUI YANG. 2004. BIFURCATIONS AND CHAOS IN TWO-CELL CELLULAR NEURAL NETWORKS WITH PERIODIC INPUTS. *International Journal of Bifurcation and Chaos* **14**:09, 3179-3204. [Abstract] [References] [PDF] [PDF Plus]
6. CHIH-WEN SHIH, CHIH-WEN WENG. 2002. ON THE TEMPLATES CORRESPONDING TO CYCLE-SYMMETRIC CONNECTIVITY IN CELLULAR NEURAL NETWORKS. *International Journal of Bifurcation and Chaos* **12**:12, 2957-2966. [Abstract] [References] [PDF] [PDF Plus]